

Discontinuum analyses of openings constructed with side drift and limited rock cover

Chia Weng BOON[†], Chee Wei NEO, David Chew Chiat NG, Victor Chee Wee ONG^{†‡}

One Smart Engineering Pte Ltd., 658065, Singapore

[†]E-mail: chiaiweng.boon@oxfordalumni.org; ong@onesmart.com.sg

Received Sept. 14, 2017; Revision accepted Feb. 9, 2018; Crosschecked Mar. 20, 2018

Abstract: The design of rock support for a typical horseshoe shaped tunnel with considerations of it being excavated into a twin arch tunnel was studied using the distinct element method (DEM). Two different competent rock covers, i.e. 4 m and 7.5 m above the tunnel crown, were analysed. The results are relevant to the granitic geological unit in Singapore which has a weathering profile with rockhead found at some locations to be only 20–35 m below ground level and undulating, leaving limited rock cover for some sections along tunnels of similar depth. The verification of the adequacy of competent rock cover is important to ensure that the choice of ground support is suitable, particularly when the tunnel is excavated using the drill-and-blast method. In the opening geometry analysed in this study, a side drift is excavated adjacent to the first tunnel to create a twin arch opening. This creates a pillar between the openings during the intermediate construction stage. The influence of excavating the side drift on the support of the first opening was studied. We found that the bolt forces in the pillar approximately doubled during the excavation of the side drift, which may have been due to the rock joint inclinations and adopted strength parameters. This paper shows how DEM analyses may be used to complement conventional empirical rock mass classifications to design rock supports. Limitations of the pressure relaxation approach to model 3D effects in 2D are acknowledged.

Key words: Rock cover; Twin tunnel; Side drift; Pillar; Distinct element method (DEM)
<https://doi.org/10.1631/jzus.A1700496>


CLC number: TU45

1 Introduction

In geological units in which the rockhead is shallow relative to the ground surface elevation, mixed face conditions are invariably encountered along some sections of underground tunnels in a mass rapid transit (MRT) project. The support method for mixed face conditions typically consists of forepoling and installation of a steel lining at the crown where soil is encountered. The lining can comprise either lattice girders or I-beams, coupled with wire mesh. At the springing where rock is encountered, rock bolting

and shotcrete lining are normally adopted for support. The finite element method and finite difference method are used widely to analyse the performance of these supports, with interests focused mainly on the support forces required in the weaker soil areas. The engineer, however, has to decide the minimum thickness of competent rock cover below which rock bolting is no longer efficient, and a support system for soil has to be adopted instead. An illustration to demonstrate the risk of limited rock cover, leading to ambiguities in designing ground support, is shown in Fig. 1. An attempt was made to assess the influence of rock cover thickness using 2D distinct element method (DEM) (Cundall, 1971). The DEM is one type of discontinuum analyses among others, namely the discontinuous deformation analyses (DDA), the numerical manifold method, and the hybrid

[‡] Corresponding author

 ORCID: Chia Weng BOON, <https://orcid.org/0000-0003-0065-7523>
© Zhejiang University and Springer-Verlag GmbH Germany, part of Springer Nature 2018

finite-discrete element method (Shi, 1988; Pine et al., 2006; He and Ma, 2010).

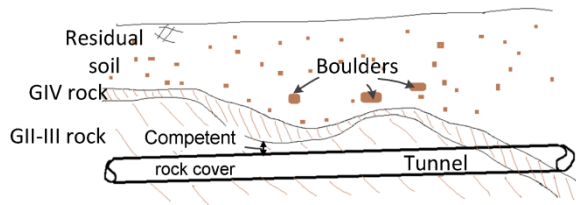


Fig. 1 Illustration to demonstrate risks related to limited competent rock cover along a tunnel alignment (indicative example)

The opening geometry in this study involved the formation of a rock pillar between the first tunnel and the side drift. Chen et al. (2009) showed that a close spacing between twin tunnels, creating a rock pillar in between the openings, can lead to larger than typical displacements, depending on the pillar width. Failure mechanisms of closely spaced tunnels in rock have also been studied by Wang and Zhu (2013) using circular DEM particles in 2D. Their results suggested that the stabilisation of pillars is important. The study of these subtleties through numerical simulations is valuable to complement conventional rock mass classifications for ground support design, such as the Q-system (Barton et al., 1974) and the rock mass rating (RMR) (Bieniawski, 1983).

The DEM, comprising polygonal blocks, was adopted in this study because it can model the stitching effects of rock bolts explicitly, whereas in the finite element and finite difference methods some equivalent continuum parameters have to be estimated and assigned as input. Continuum analyses are more widely adopted due to their shorter computation time and familiarity among engineers, although some precautions have to be exercised (Sakurai, 2009). Note that the DEM has been adopted in other rock excavation projects to verify stress concentrations of rock bolts at rock joints, and to detect potential adverse geological conditions due to unfavourable fracture orientations relative to the tunnel opening (Barton et al., 1994; Bandis, 2004). The DEM is now a common tool for cavern design (GEO, 2012). The presence of fractures in a rock cover of limited thickness may be an important engineering consideration as it may affect the type and arrangement of the support, and it could be studied effectively using this numerical method.

2 Background problem and model

The DEM code YADE was used (Kozicki and Donze, 2008; Smilauer, 2015). The algorithms developed for the DEM simulations are explained by Boon (2013) and Boon et al. (2012, 2015c). Verifications of the numerical code on ground support design have been reported by Boon et al. (2015b). Validations using a jointed beam model and a rock slide case history have been detailed in (Boon et al., 2014, 2015a).

The geometry of the first tunnel is horseshoe shaped with a diameter of about 12 m, and with an adjacent drift opening finally forming a twin-arch. A pillar is created between the first tunnel and the side drift. In the final construction stage, the pillar is excavated after the permanent lining of the first tunnel is erected. The study here included the excavation of the side drift, before the creation of the twin-arch. The model does not refer to a specific case history, but relates generally to the need to excavate wide span openings, for instance to accommodate an additional track, e.g. a cripple siding in an MRT project, where cut-and-cover is not feasible due to logistic reasons in an urban environment.

The tunnel centre is about 30 m below ground level, with 24 m of cover above the crown. The apparent dip angles of the joint sets observed at the tunnel face are 80° (subvertical) and -45° (inclined with dip direction opposite to the previous joint set) (Fig. 2). This is an idealisation in terms of analyses because in a real situation the apparent dip angle may change along the tunnel alignment. The average block size of the GIII rock is between 1 and 2 m. References for the weathering grade of rock in the Bukit Timah Granite in Singapore can be found in (Zhao et al., 1994a, 1994b). The shear stiffness of the rock joint was estimated based on the block size and the estimated stress range (Bandis et al., 1983; Barton, 2016) (Fig. 3). The adopted rock joint normal stiffness was 5 GPa/m and rock joint shear stiffness was 0.5 GPa/m. The latter takes into account potential scale effects which will result in smaller values than those measured in the laboratory (i.e. block size is considered in the x-axis of Fig. 3). Note that these stiffness values were estimated, and should not be

cited as representative of the local geology. Details of the Singapore geology can be found in (Zhao et al., 1994a, 1994b, 1995; Zhou et al., 2003). The rock joint friction angle was adopted as 35° . The adopted horizontal to vertical stress ratio, K_0 , was 0.8. The adopted rock properties for the DEM simulations are summarised in Table 1. The rock bolt length was 4.5 m, unless otherwise mentioned. The stiffness of the rock bolt was 0.1 GN/m based on estimates in (Stillborg, 1994) for Swellex bolts. Details of the mechanics

Table 1 Rock parameters adopted in the DEM simulation

Parameter	Value
Rock joint normal stiffness, k_n (GPa/m)*	5
Rock joint shear stiffness, k_s (GPa/m)*	0.5
Friction angle ($^\circ$)	35
Horizontal to vertical stress ratio, K_0	0.8
Block size for GIII rock (m)	1–2
Rock joint dip angles for two joint sets ($^\circ$)	80, –45

* Estimated values based on discussion in the main text (not from local experimental data)

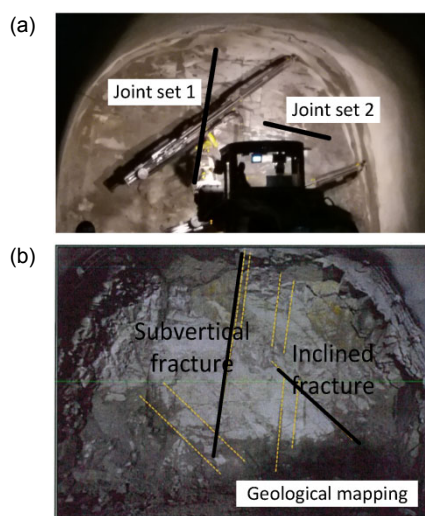


Fig. 2 Jointed granitic unit with two main joint sets visible at the tunnel face: (a) rock bolt installation; (b) face mapping

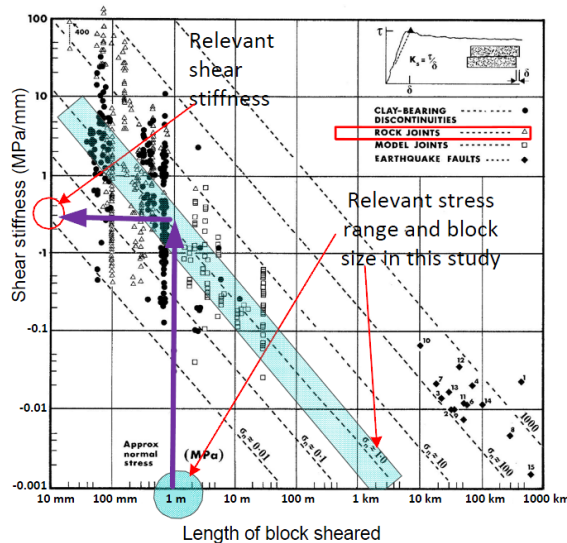


Fig. 3 Adopted shear stiffness for modelling based on the typical geological conditions. Annotated and modified after Bandis et al. (1983), Copyright 1983, with permission from Elsevier

of inflatable bolts can be found in (Li, 2016). Simplifications of the rock bolt mechanism were made, as discussed in Boon et al. (2015b). The rock bolt resistance in the DEM analyses was assumed to be concentrated along rock discontinuities only and the bolt was assumed to be fully rigid within the rock blocks. A shotcrete thickness of 0.3 m was adopted in the model. Similar (non-identical) geological profiles and tunnel geometries are known to exist in recent MRT projects in Singapore. An annotated screen capture of the model, including its boundaries, is shown in Fig. 4a.

It is important to acknowledge the assumptions in the 2D model; for instance, 3D effects in terms of the longitudinal displacement profile have been simplified in the 2D model, i.e. making reference to typical longitudinal profiles studied by Panet (1993), Chern et al. (1998), and Vlachopoulos and Diederichs (2009). The magnitude of relaxation depends on the distance of bolt installation from the advancing face (Fig. 2a). The stages of the simulations are summarised in a flowchart shown in Fig. 4b. In principle, the use of 3D models, for instance as showcased by Ong and Ng (2014), is more direct. In the simulations here, the internal pressure acting at the tunnel opening in the 2D model, before the support is installed, was initially assigned to be the same as the overburden pressure p_0 , and was allowed to relax to $0.7p_0$ before support installation (relaxation ratio of 0.3), where p_0 is the overburden pressure. We assumed that the modelling approach of reducing the internal pressure in 2D is more conducive to allowing the tunnel opening and boundary conditions (rock cover in this case) to interact, compared to prescribing the internal strains or volume loss induced by tunnelling (Boon and Ooi, 2016). Due to limitations of the numerical

code to model multiple stages of temporary lining, the opening was not modelled by stages, i.e. advancement of the heading and bench, but was excavated in one instant, with the support installed later at $0.7p_0$ for the opening. Excavation of the opening in one instant may slightly affect the stress distribution around the ground support. After support installation, the internal pressure was removed. We assumed that the support was temporary and dry, and the lining was not subject to water pressure. It is noted that the assumption that the lining was effective in support contribution would in practice require satisfactory evaluation of the lining installation details.

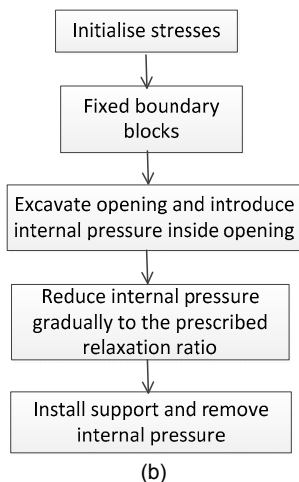
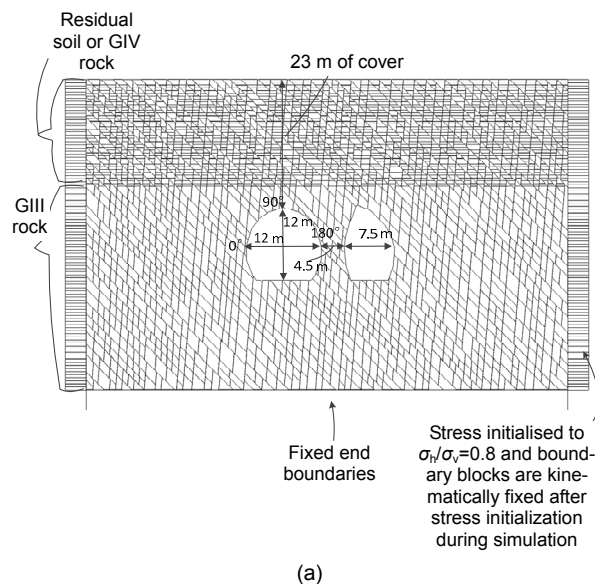


Fig. 4 Description of the numerical model

(a) Annotations showing boundary conditions; (b) Flow chart showing stages of simulations for excavating an opening

3 Results and discussion

Two thicknesses of competent GIII rock cover were investigated, namely 4 m and 7.5 m thick (Figs. 5a and 5b). These two rock covers were adopted for analyses because they relate well to the tunnel diameter size (less than half and more than half, respectively), and are within the range of lengths commonly used for rock support. The GIV rock and residual soil material were modelled using smaller sized blocks to mimic material with lower resistance in the numerical code. The excavation of the side drift adjacent to the first tunnel before forming a twin arch was also investigated (Fig. 6). The results are presented in the following order: (i) failure mechanisms, (ii) support requirements of a single tunnel, and (iii) increase in support requirements due to the adjacent excavation of the side drift. The rock bolts are identified using angles defined in Fig. 5a.

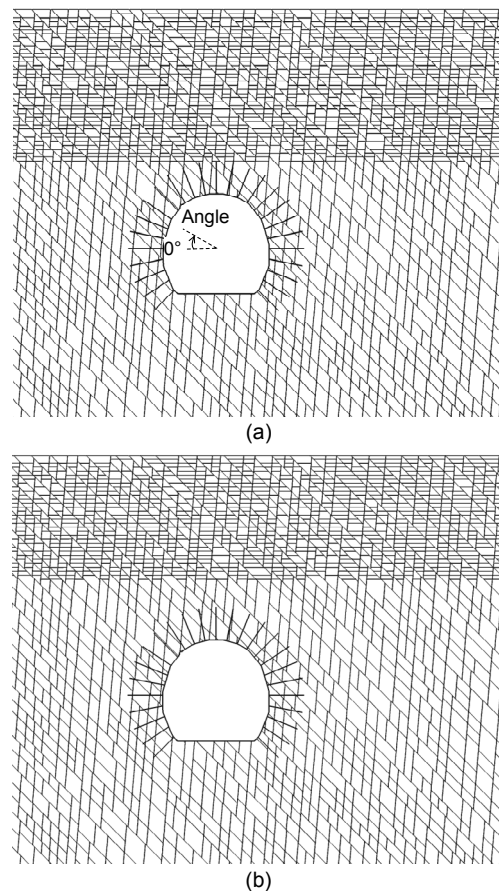


Fig. 5 DEM model with different competent rock cover (a) 4 m (dashed horizontal line shows reference axis with zero degree, and angle increases clockwise) and (b) 7.5 m GIII rock

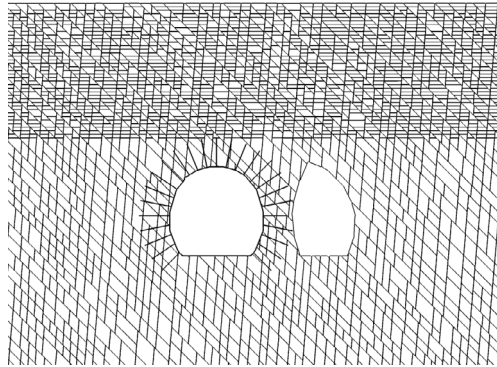


Fig. 6 DEM model with excavation of side drift adjacent to the first tunnel (the side drift on the right is supported by internal pressure)

3.1 Failure mechanisms

The failure mechanism of the single tunnel was investigated by modelling an unsupported opening, and the results are shown in Fig. 7. We found that the fractures in the rock mass governed the failure mechanisms as they act as planes of weakness. The initial loosening propagated into a larger roof collapse. In the second analysis, the first tunnel was supported with internal pressure and the adjacent side drift was excavated and unsupported. We found that the pillar between the tunnels comprising smaller blocks slid into the side drift (Fig. 8).

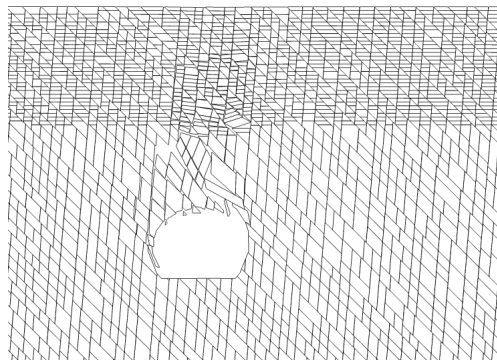


Fig. 7 Failure mechanism governed by joint sets at the roof

3.2 Results with different rock cover

For the case when the GIII rock cover above the tunnel crown was reduced from 7.5 m to 4 m, the rock bolt forces increased by from 3% to 9% (Fig. 9), whereas the lining forces increased by about 3%–6% (Fig. 10). The predicted displacements after support installation were in the range of 2–3 mm (Fig. 11).

When the displacements before support installation were incorporated, the total displacements were in the range of 8–9 mm. Note that examination of the support forces alone (i.e. Figs. 9 and 10) may not reveal the full engineering risks, particularly in the

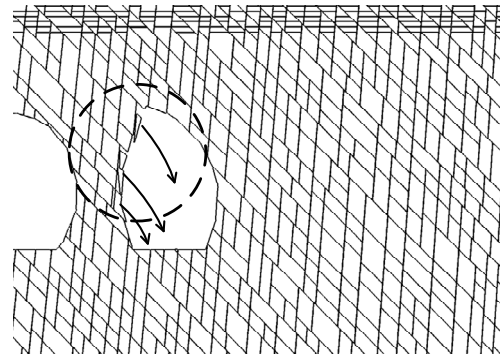


Fig. 8 Failure mechanism governed by joint sets at the pillar when excavating the adjacent tunnel (the first tunnel is supported by internal pressure, and the second (drift) tunnel on the right is unsupported)

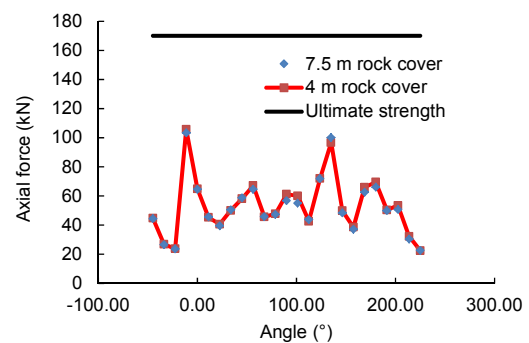


Fig. 9 Bolt forces with different GIII rock cover (capacity based on DSI-OMEGA friction bolts (EFB-160 type); refer to Fig. 5a for orientation of angles)

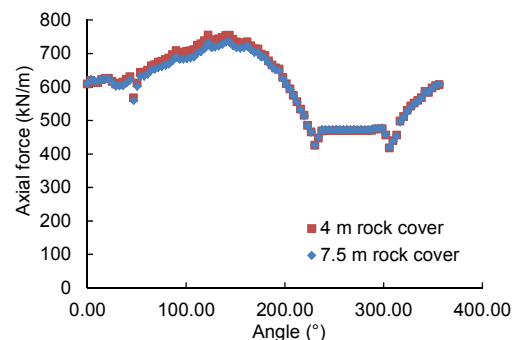


Fig. 10 Lining axial forces with different GIII rock cover (refer to Fig. 5a for orientation of angles)

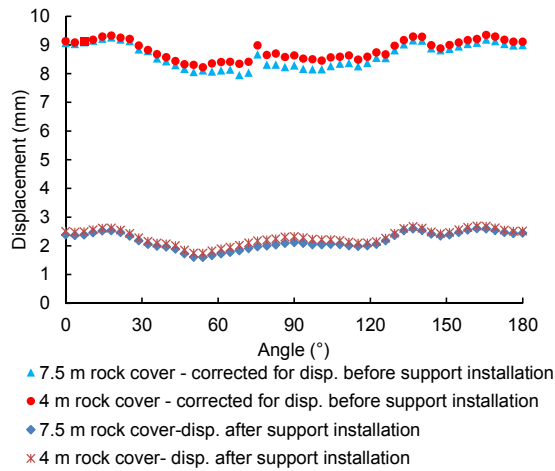


Fig. 11 Displacement of opening for different GIII rock covers for the case after support installation of the first opening and the case after correction to include the displacements before support installation

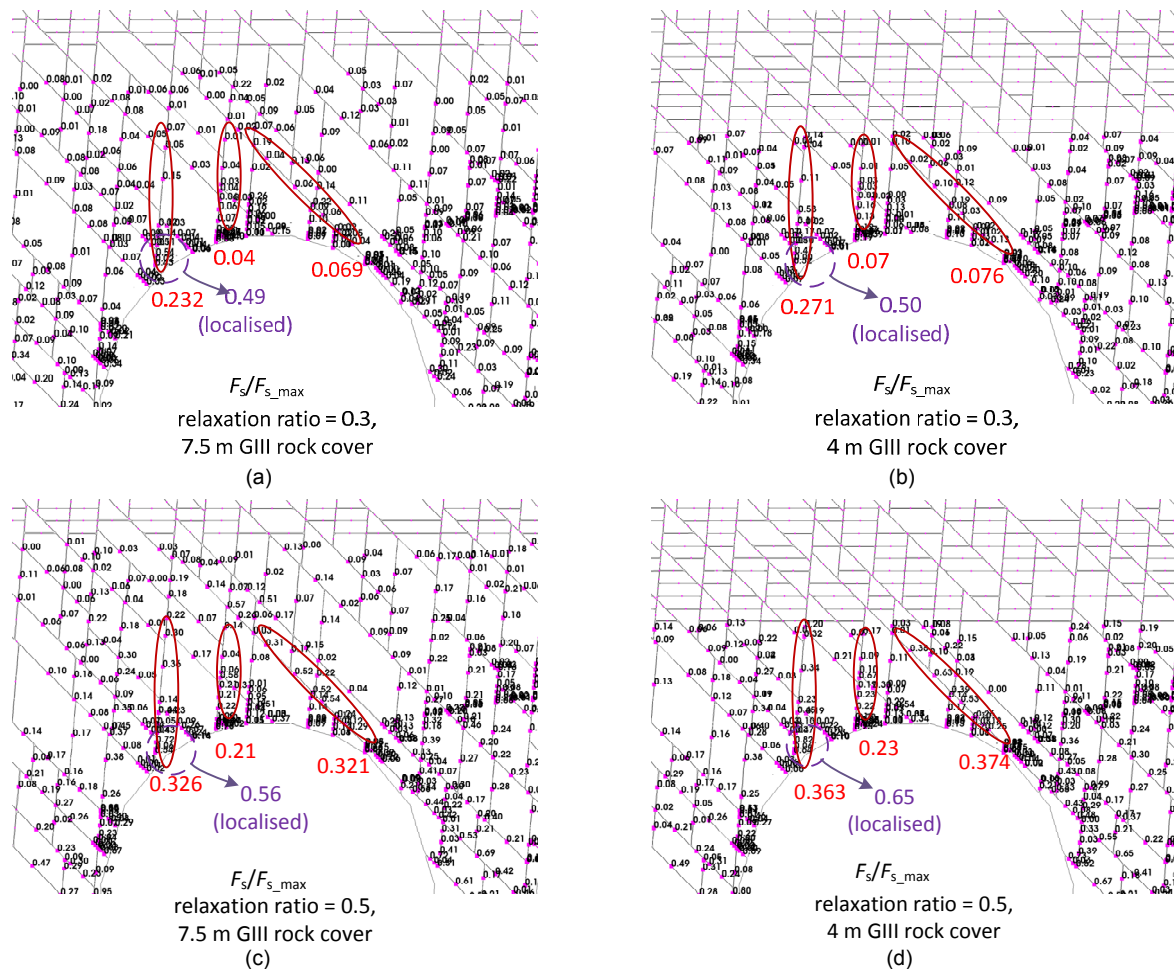


Fig. 12 Comparison of averaged mobilised resistance on potential sliding planes for relaxation ratio of 0.3 with rock cover 7.5 m (a) and 4 m (b), and for relaxation ratio of 0.5 with rock cover 7.5 m (c) and 4 m (d). Numbers in the figures are the mobilised resistance normalised by the frictional resistance. Numbers in larger font size represent the average mobilisation ratio of the area circled or highlighted

temporary condition before support installation. For instance, Boon et al. (2015b) found that the bolt forces increased marginally only when the rock mass is not adequately supported, with ravelling of blocks taking place between the bolts.

Since most displacements occurred before support installation, it was important to examine the stresses in the jointed rock structure in the temporary condition before support installation. This was an important procedure at least to counter-verify that the internal distribution of mobilised resistance along potential sliding planes of roof blocks corresponded approximately to the assumed relaxation applied at the internal boundary. Two scenarios with $0.7p_0$ and a lower bound of $0.5p_0$ of internal pressure (relaxation ratios of 0.3 and 0.5, respectively) were examined (Fig. 12). The mobilised resistance normalised by

the frictional resistance for each contact along the three selected potential sliding planes (circled) were averaged and are annotated in the figures (with larger font). The reduced rock cover from 7.5 m to 4 m led to an increase in the mobilised resistance ratio of 10%–17% within the same thickness of rock layer for the case with a relaxation ratio of 0.5 (Figs. 12c and 12d). Note that there were also localised areas with a higher mobilised resistance ratio than the prescribed relaxation ratio applied at the internal boundary (dashed circles in Fig. 12 close to the tunnel opening).

3.3 Impact of adjacent excavation onto the first tunnel

After the first tunnel was excavated and supported, the excavation of the side drift was simulated. It was not straightforward to assume a relaxation ratio, and the internal pressures at the side drift were relaxed gradually to $0.7p_0$ and $0.5p_0$ for sensitivity analyses (i.e. relaxation ratios of 0.3 and 0.5, respectively). The reason is that the confinement around the side drift had been reduced due to the presence of the first tunnel. A large internal pressure may result in the applied pressure causing active expansion instead of allowing deformations to take place in a passive manner. The differences between these two assumptions of relaxation ratios were found to be minor. The larger relaxation ratio (applied at the side drift) of 0.5 compared to 0.3 resulted in increased convergence of the first tunnel in most areas, apart from angles 150° – 210° close to the pillar (Fig. 13) where slightly smaller convergence was observed. We believe this was due to the increased tendency of the blocks to move into the side drift and away from the first tunnel. Note that the displacements shown in Fig. 13 are the displacements of the tunnel lining which is at the periphery of the opening and they do not represent the overall movement of the blocks around the opening. Note that the lining nodal displacements may not be fully compatible with the nearest rock block, as the lining nodes need to respond to the external forces in an integral manner, and separation between the lining nodes and rock blocks is possible. Note that, before embarking on numerical analyses in practice, the assumption that the lining is providing substantial support has to be checked against the actual extent of the lining that would be installed around the opening in the field.

Due to the adjacent excavation, the bolt forces at the pillar approximately doubled in magnitude (diamond and crosses compared to squares in Fig. 14). The lining axial forces increased by about 6%, and the bending moments were also found to increase by small amounts (Figs. 15a and 15b). From Fig. 15c, the 300 mm thick lining could potentially be optimised, but this was not pursued in this study.

The additional increase in movement in the first tunnel due to the excavation of the side drift was found to be in the range of 1 mm and was

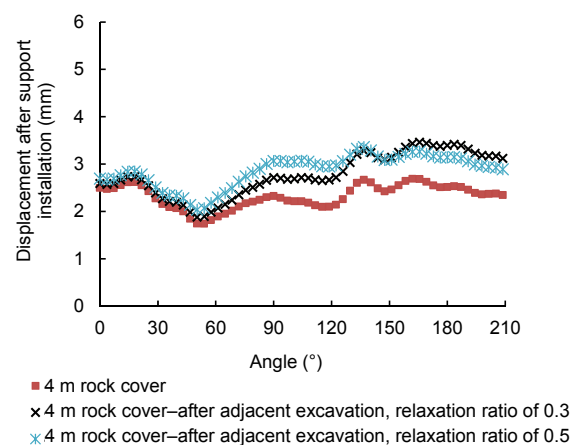


Fig. 13 Increase in lining displacements of the first tunnel due to adjacent excavation of the side drift with internal pressure relaxation ratio of 0.3 and 0.5. Refer to Fig. 5a for orientation of angles

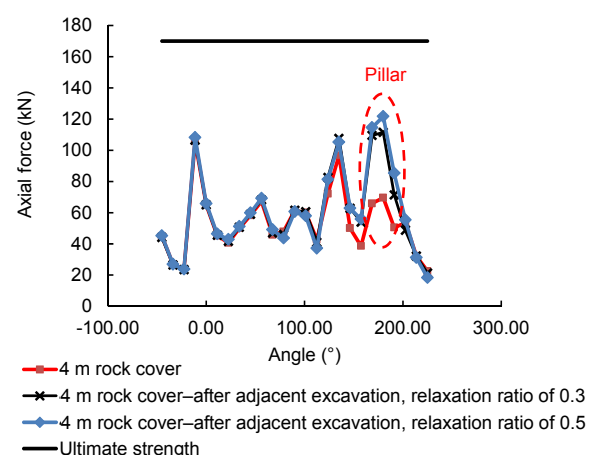


Fig. 14 Increase in bolt forces due to excavation of the adjacent side drift with internal pressure relaxation ratio of 0.3 and 0.5. Estimated ultimate strength based on DSI-OMEGA friction bolts (EFB-160 type). Refer to Fig. 5a for orientation of angles

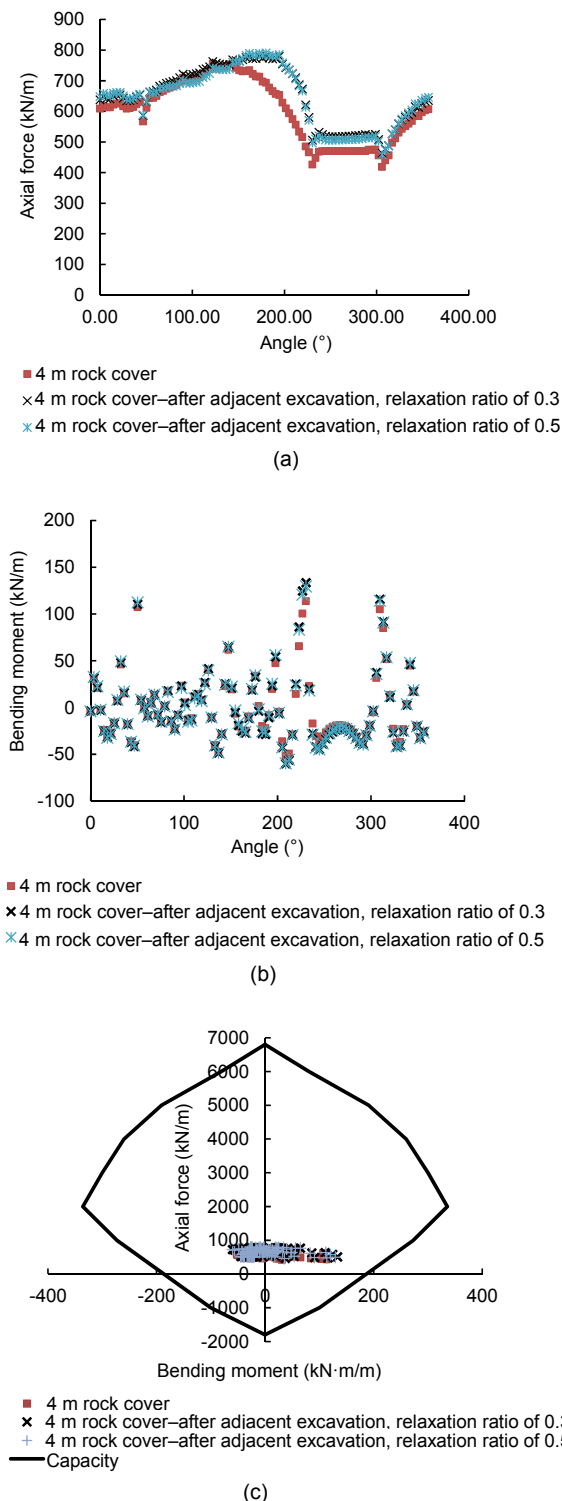


Fig. 15 Increase in lining forces due to excavation of the adjacent side drift: (a) axial force; (b) bending moment; (c) Axial force-bending moment plot based on capacity of 300 mm-thick shotcrete lining and wire mesh of $\Phi 13$ mm/150 mm-150 mm. Refer to Fig. 5a for orientation of angles

concentrated at the wall closer to the side drift (Fig. 13). The total maximum movement was about 3.5 mm. As discussed in the beginning of Section 2, the installation of the permanent lining and subsequent removal of the pillar to form a twin-arch was not studied (Fig. 16). This was due to limitations of the numerical code in modelling permanent structures.

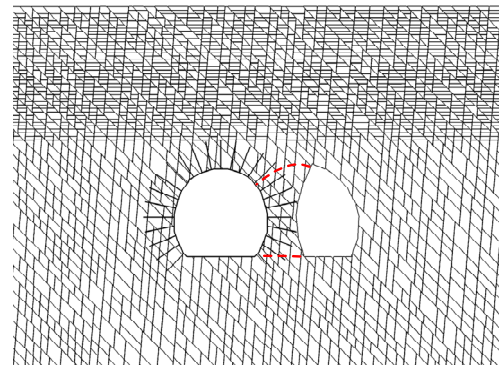


Fig. 16 Twin arch geometry. Dashed lines indicate final excavation boundaries

4 Conclusions

When excavating large span openings underground, for instance to accommodate an additional track as a cripple siding in an MRT tunnel, the construction sequence commonly involves excavating a single tunnel first, followed by a side drift, thereby creating a pillar between the tunnels. The tunnel geometry analysed here is also relevant to closely spaced twin tunnels. This problem was investigated under limited rock cover conditions using the distinct element method with polygonal blocks. The removal of the pillar after the installation of the permanent concrete structure was not studied.

Note that the numerical results reported here are not universal and are limited to the block size, opening geometry, in-situ stresses, and rock joint parameters adopted in the DEM analyses. As the definition of rock grade in the discussion depends on the classification provided by the engineering geologist after inspecting the exposed surface, an assessment will need to be made on a case to case basis at different sites to ensure that the modelling assumptions are compatible with the actual rock mass conditions. The

degree of fracturing and other factors in the rock mass classifications (Q-system and RMR) should also be considered at the same time. For an opening size of about 12 m and average block size of 1.5 m, a reduced GIII rock cover of 4 m thickness compared to 7.5 m thickness was found to result in marginally larger support forces, with differences in the range of 3%–9%, for a single tunnel. Before support installation, both the local and larger scales of stabilities within the rock structure have to be assessed. For a conservative relaxation ratio of 0.5 before support installation, the mobilisation ratios averaged along potential sliding planes were found to increase by 10%–17% when the GIII rock cover reduced from 7.5 m to 4 m. The actual magnitudes of averaged mobilisation ratios appeared to be within acceptable limits, with larger mobilisation ratios around individual rock blocks. Typically, encountered loose blocks have to be carefully scaled off in a controlled manner. The increase in mobilisation ratios may be greater for weaker rock joint parameters, although this was not studied in further detail. This is an important consideration when evaluating the safety of a tunnel in the temporary condition before any engineering support is in place. Tunnelling construction procedures such as the control of the advance length, unsupported length, and probing ahead of the tunnel face become more critical when the rock cover is reduced.

When the side drift was excavated adjacent to the first tunnel, the displacements and forces of the bolts (away from the rock pillar) and shotcrete lining were found to increase marginally, and they were within the capacities of the support. Limitations of the pressure relaxation approach for simulating an adjacent excavation are acknowledged and discussed briefly in the main text. From the results, however, it was found that the bolt forces at the pillar approximately doubled, suggesting that in practice it may be necessary to provide additional rock bolt or tie reinforcement to strengthen the pillar. This may depend on the rock joint inclinations and strength parameters (no cohesion and no dilation) adopted in the analyses. Note that the choice of excavation sequence between the horseshoe tunnel and the side drift opening in an anisotropic rock mass (governed by the joint inclina-

tions) may potentially affect the interactions between the openings.

Finally, the analyses here assumed that the analysed rock covers existed in plane strain, and 3D effects were not addressed in a very rigorous manner. Other considerations, such as the rockhead profile ahead of the tunnel face and other geological features, also play an important factor in practice, since a reduction in rock cover may affect both the face and roof stability. Nonetheless, this study demonstrates how 2D DEM analyses may be used to complement routine rock mass classifications, such as the Q-system or RMR, in terms of quantifying the influence of reduced rock cover and an adjacent tunnel on the rock support.

Acknowledgements

The work was undertaken at One Smart Engineering Pte Ltd., Singapore in 2016. The authors would like to thank the organisation for the encouragement. The analyses presented here do not indicate a preference for the numerical methods by the institutions to which the authors are affiliated.

References

- Bandis SC, Lumsden AC, Barton NR, 1983. Fundamentals of rock joint deformation. *International Journal of Rock Mechanics and Mining Sciences & Geomechanics Abstracts*, 20(6):249-268.
[https://doi.org/10.1016/0148-9062\(83\)90595-8](https://doi.org/10.1016/0148-9062(83)90595-8)
- Barton N, 2016. Empirical methods, rock mechanics, and structural geological methods useful for excavation in jointed/fractured media. Short Course Notes in EUROCK 2016.
- Barton N, Lien R, Lunde J, 1974. Engineering classification of rock masses for the design of tunnel support. *Rock Mechanics*, 6(4):189-236.
<https://doi.org/10.1007/BF01239496>
- Barton N, By TL, Chrysanthakis P, et al., 1994. Predicted and measured performance of the 62-m span Norwegian Olympic Ice Hockey Cavern at Gjøvik. *International Journal of Rock Mechanics and Mining Sciences & Geomechanics Abstracts*, 31(6):617-641.
[https://doi.org/10.1016/0148-9062\(94\)90004-3](https://doi.org/10.1016/0148-9062(94)90004-3)
- Bieniawski ZT, 1983. Geomechanics classification (RMR system) in design applications to underground excavations. Proceedings of the International Symposium on Engineering Geology and Underground Construction.
- Boon CW, 2013. Distinct Element Modelling of Jointed Rock Masses: Algorithms and Their Verification. PhD Thesis, University of Oxford, UK.

- Boon CW, Ooi LH, 2016. Tunnelling past critical structures in Kuala Lumpur: insights from finite element analyses and TZ load transfer analyses. *Geotechnical Engineering Journal of the SEAGS & AGSSEA*, 47(4):109-122.
- Boon CW, Houlsby GT, Utili S, 2012. A new algorithm for contact detection between convex polygonal and polyhedral particles in the discrete element method. *Computers and Geotechnics*, 44:73-82.
<https://doi.org/10.1016/j.compgeo.2012.03.012>
- Boon CW, Houlsby GT, Utili S, 2014. New insights into the 1963 Vajont slide using 2D and 3D distinct element method analyses. *Géotechnique*, 64(10):800-816.
<https://doi.org/10.1680/geot.14.P.041>
- Boon CW, Houlsby GT, Utili S, 2015a. DEM modelling of a jointed beam with emphasis on interface properties. *Géotechnique Letters*, 5(1):49-55.
<https://doi.org/10.1680/geolett.14.00105>
- Boon CW, Houlsby GT, Utili S, 2015b. Designing tunnel support in jointed rock masses via the DEM. *Rock Mechanics and Rock Engineering*, 48(2):603-632.
<https://doi.org/10.1007/s00603-014-0579-8>
- Boon CW, Houlsby GT, Utili S, 2015c. A new rock slicing method based on linear programming. *Computers and Geotechnics*, 65:12-29.
<https://doi.org/10.1016/j.compgeo.2014.11.007>
- Chen SL, Lee SC, Gui MW, 2009. Effects of rock pillar width on the excavation behaviour of parallel tunnels. *Tunnelling and Underground Space Technology*, 24(2):148-154.
<https://doi.org/10.1016/j.tust.2008.05.006>
- Chern JC, Shiao FY, Yu CW, 1998. An empirical safety criterion for tunnel construction. Proceedings of the Regional Symposium on Sedimentary Rock Engineering, p.222-227.
- Cundall PA, 1971. A computer model for simulating progressive, large scale movement in blocky rock system. ISRM Symposium, 2:129-136.
- GEO (Geotechnical Engineering Office), 2012. GEO Technical Guidance Note No. 32 (TGN 32) Updating of Geoguide 4—Guide to Cavern Engineering. Geotechnical Engineering Office, Civil Engineering and Development Department, The Government of Hong Kong Special Administrative Region, China.
- He L, Ma G, 2010. Development of 3-D numerical manifold method. *International Journal of Computational Methods*, 7:107-129.
- Kozicki J, Donze FV, 2008. A new open-source software developed for numerical simulations using discrete modelling methods. *Computer Methods in Applied Mechanics and Engineering*, 197(49-50):4429-4443.
<https://doi.org/10.1016/j.cma.2008.05.023>
- Li CC, 2016. Analysis of inflatable rock bolts. *Rock Mechanics and Rock Engineering*, 49(1):273-289.
<https://doi.org/10.1007/s00603-015-0735-9>
- Ong VCW, Ng DCC, 2014. Overview of design and construction of deep excavation and tunnelling projects in Singapore. Seminar Organised by the Tunnelling and Underground Space Technical Division (TUSTC), The Institution of Engineers Malaysia (IEM), Malaysia.
- Panet M, 1993. Understanding deformations in tunnels. In: Hudson JA, Brown ET, Fairhurst C, et al. (Eds.), *Comprehensive Rock Engineering*, Vol. 1. Pergamon, London, UK, p.663-690.
- Pine RJ, Coggan JS, Flynn ZN, et al., 2006. The development of a new numerical modelling approach for naturally fractured rock masses. *Rock Mechanics and Rock Engineering*, 39(5):395-419.
<https://doi.org/10.1007/s00603-006-0083-x>
- Sakurai S, 2009. Discussion on the problems in modelling jointed rock reinforced by rock bolts in tunnels. ISRM SINOROCK 2009, p.36-40.
- Shi GH, 1988. Discontinuous Deformation Analysis: a New Numerical Model for the Statics and Dynamics of Block Systems. PhD Thesis, University of California, Berkeley, USA.
- Smilauer V, 2015. Yet Another Dynamic Engine (YADE) Documentation, 2nd Edition. The YADE Project.
- Stillborg EB, 1994. Professional Users Handbook for Rock Bolting, 2nd Edition. Trans Tech Publications Limited.
- Vlachopoulos N, Diederichs MS, 2009. Improved longitudinal displacement profiles for convergence confinement analysis of deep tunnels. *Rock Mechanics and Rock Engineering*, 42(2):131-146.
<https://doi.org/10.1007/s00603-009-0176-4>
- Wang C, Zhu H, 2013. Study on the failure mechanism of small spacing tunnels by DEM. Proceedings of the 3rd ISRM SINOROCK Symposium: Rock Characterisation, Modelling and Engineering Design Methods, p.613-616.
- Zhao J, Broms BB, Zhou Y, et al., 1994a. A study of the weathering of the Bukit Timah Granite Part A: review, field observations and geophysical survey. *Bulletin of the International Association of Engineering Geology*, 49(1): 97-106.
<https://doi.org/10.1007/BF02595006>
- Zhao J, Broms BB, Zhou Y, et al., 1994b. A study of the weathering of the Bukit Timah Granite Part B: field and laboratory investigations. *Bulletin of the International Association of Engineering Geology*, 50(1):105-111.
<https://doi.org/10.1007/BF02594962>
- Zhao J, Zhou Y, Sun J, et al., 1995. Engineering geology of the Bukit Timah Granite for cavern construction in Singapore. *Quarterly Journal of Engineering Geology and Hydrogeology*, 28(2):153-162.
<https://doi.org/10.1144/GSL.QJEGH.1995.028.P2.06>
- Zhou Y, Zhao J, Cai JG, et al., 2003. Behaviour of large-span rock tunnels and caverns under favourable horizontal stress conditions. Proceedings of ISRM 2003—Technology Roadmap for Rock Mechanics, South African Institute of Mining and Metallurgy, p.1381-1386.

中文概要

题目: 关于具有侧边导坑和有限岩石覆盖层的隧道开口的离散分析

目的: 针对新加坡的花岗岩地质结构, 研究将典型马蹄形隧道挖掘成双拱隧道时岩石支撑的设计问题。利用离散元法分析侧边导坑对隧道主体开口的影响。

创新点: 1. 基于平面应变假设, 提出一个针对性的离散元模型以分析侧边导坑的设置对主体隧道支撑的影响; 2. 此模型适用于解决底下长跨度开口的支

撑设计问题, 如大众捷运系统隧道和紧贴式双孔隧道的建造, 补充了传统经验主义的设计方法。

方法: 1. 采用离散元法对马蹄形隧道开口支撑问题进行非连续分析; 2. 采用二维平面应变模型简化问题。

结论: 1. 离散元法可用于分析有限岩石覆盖层的失效机制, 单隧道支撑要求以及增加侧边导坑后的支撑要求; 2. 模型计算结果显示, 侧边导坑的挖掘使得支柱总的螺栓连接作用力增加了一倍。

关键词: 岩石覆盖层; 双隧道; 侧边导坑; 支柱; 离散元法